Wang et al. Nanoscale Research Letters 2014, 9:624
http://www.nanoscalereslett.com/content/9/1/624

Nanoscale Research Letters
a SpringerOpen Journal

NANO EXPRESS Open Access

Surfactant-free synthesis of Cu_2O hollow spheres and their wavelength-dependent visible photocatalytic activities using LED lamps as cold light sources

Yuxi Wang[1], Da Huang[1], Xingzhong Zhu[1], Yujie Ma[1], Huijuan Geng[1], Ying Wang[1], Guilin Yin[2], Dannong He[2], Zhi Yang[1,2*] and Nantao Hu[1*]

Abstract

A facile synthesis route of cuprous oxide (Cu_2O) hollow spheres under different temperatures without the aid of a surfactant was introduced. Morphology and structure varied as functions of reaction temperature and duration. A bubble template-mediated formation mechanism was proposed, which explained the reason of morphology changing with reaction temperature. The obtained Cu_2O hollow spheres were active photocatalyst for the degradation of methyl orange under visible light. A self-designed equipment of light emitting diode (LED) cold light sources with the wavelength of 450, 550, and 700 nm, respectively, was used for the first time in the photocatalysis experiment with no extra heat introduced. The most suitable wavelength for Cu_2O to photocatalytic degradation is 550 nm, because the light energy (2.25 eV) is closest to the band gap of Cu_2O (2.17 eV). These surfactant-free synthesized Cu_2O hollow spheres would be highly attractive for practical applications in water pollutant removal and environmental remediation.

Keywords: Cuprous oxide; Hollow spheres; Surfactant-free; Photocatalysis; LED cold light sources

Background

Recently, semiconductor nanomaterials with different morphologies have attracted lots of interests because structure significantly influences their physical and chemical properties. Various morphologies, such as nanowires [1], nanocubes [2], nanocages [3], and octahedrons [4], have been synthesized for their interesting properties and applications. Among these nanostructures, hollow nanostructures are of particular interest because of their unique electrical, magnetic, thermal, and optical properties [5-13]. Hollow nanomaterials are widely used as nanoscale chemical reactors [14], high-performance catalysts [14-16], drug-delivery carriers [17,18], lithium-ion battery materials [19], and wavelength optical components for biomedical applications [20]. According to the reports related to the preparation of hollow materials, various methods have been developed which can be categorized into the following classes: template-mediated approaches [21], chemical etching [22], galvanic replacement [23], and the Kirkendall voiding [6]. Among the above methods mentioned, template-mediated approaches are the most usual and popular ones, which are based on selectively removing the cores in spherical core-shell particles by a solvent or calcination method.

Cuprous oxide (Cu_2O), a typical p-type semiconductor with a direct band gap of 2.17 eV, has been broadly applied in photocatalysis [24], gas sensors [8,25], solar cells [26,27], photoelectrochemical cells [28,29], and lithium-ion batteries [19]. It is noticed that Cu_2O with different shapes have attracted much attention. Many efforts have been made to obtain Cu_2O nanomaterials [30]. Wet chemical reduction [31-35], electrodeposition [11,12,36-38], solvothermal synthesis [39-41], and irradiation [42,43] methods have been applied to prepare Cu_2O nanocrystals. However,

* Correspondence: zhiyang@sjtu.edu.cn; hunantao@sjtu.edu.cn
[1]Key Laboratory for Thin Film and Microfabrication of Ministry of Education, Department of Micro/Nano Electronics, School of Electronic Information and Electrical Engineering, Shanghai Jiao Tong University, Shanghai 200240, People's Republic of China
[2]National Engineering Research Center for Nanotechnology, Shanghai 200241, People's Republic of China

the reported synthetic routes are relatively complex and time consuming, typically involving expensive toxic solvents and surfactants, which make it difficult to purify as-produced Cu_2O hollow nanostructure as well as produce it in large scale [25,44-46]. Therefore, it is highly rewarding to facile synthesize functional Cu_2O nanomaterials in a solution without a surfactant.

Meanwhile, Cu_2O photocatalyst can convert solar into chemical energy to degrade pollutants and can be used as a promising catalyst for environmental wastewater treatment in practical application [24]. Xe lamps and high-pressure mercury lamps with the power of 150 and 400 W, respectively, are usually used as light sources in photocatalytic experiment. They will introduce large amount of heat into the catalytic system, which makes it difficult to control the reaction temperature.

Herein, we investigate Cu_2O hollow spheres via a facile aqueous solution method under different temperatures without the addition of a surfactant. In our research, hollow spheres with uniform diameter can be obtained through this surfactant-free method. Morphologies of Cu_2O hollow spheres prepared under different temperatures are displayed and so does the supposed formation mechanism. In addition, photocatalytic activities of Cu_2O hollow spheres are measured for the first time with a self-designed equipment using light emitting diode (LED) cold lamps with different characteristic wavelengths as photocatalysis light source. LED lamps with the power of 8 W, as typical cold light sources, are different from the high-power Xe lamps and mercury vapor lamps. There is no extra heat introduced into the catalytic system using LED cold light and the wavelength can be easily controlled. This one-pot method proceeds in aqueous medium with low temperatures and high reaction rates, which makes the as-produced Cu_2O hollow spheres highly attractive for practical applications in water pollutant removal and environmental remediation.

Methods

Materials

Copper sulfate pentahydrate ($CuSO_4 \cdot 5H_2O$) and hydrazine hydrate ($N_2H_4 \cdot H_2O$) are purchased from Sinopharm Chemical Reagent Co., Ltd. (Shanghai, China), of analytical grade, and used without further purification.

Preparation of Cu_2O hollow spheres

In a typical synthesis, 0.25 g of $CuSO_4 \cdot 5H_2O$ were dissolved in 50 mL of deionized water with continuous stirring. Then, the transparent solution was kept in a 100-mL flask under different temperatures. We used $N_2H_4 \cdot H_2O$ (20%) to reduce Cu^{2+} by fast injection of 1 mL $N_2H_4 \cdot H_2O$ into the solution and stirring at 750 rpm for 1 h. The color of the solution turned from dark blue to brick red with no extra alkali added. After that, the product was centrifuged at 3,250 × g for 10 min, washed with deionized water for several times, and finally dried in a vacuum at 60°C for 8 h.

Photocatalytic activities

Photocatalytic degradation of methyl orange (MO) was carried out in a self-designed equipment. Twenty milligrams of as-prepared Cu_2O hollow spheres and 50 mL MO solution (10 mg/L) were kept in a 100-mL round-bottom flask with continuous stirring. Four 8-W LED lamps with the same characteristic wavelengths (450, 550, or 700 nm) were used for the first time as cold light sources which were mounted at 10 cm around the solution. Vigorous stirring was employed to ensure the adsorption equilibrium and eliminate any diffusion effect. The MO solution was kept in darkness for 15 min to get adsorption equilibrium and then under visible light.

Characterizations

The sample sizes and morphologies were investigated using scanning electron microscope (SEM) and transmission electron microscope (TEM). SEM images were performed with a Carl Zeiss Ultra 55 from Carl Zeiss AG, Oberkochen, Germany. TEM images were obtained with a JEOL JEM-2100 TEM operating at 200 kV from JEOL Ltd., Akishima, Tokyo, Japan. The crystal structures were examined by X-ray diffractometer (XRD; D8 Advance, Bruker, Ettlingen, Germany) with Cu Kα (λ =1.5418 Å) and 2θ from 20° to 80°. Ultraviolet–visible spectra (UV–vis, Lambda 500, PerkinElmer, Waltham, MA, USA) characterizations were carried out at the region from 350 to 600 nm. Nitrogen adsorption-desorption isotherms were collected on an autosorb-iQA3200-4 sorption analyzer (Quantatech Co., New York, NY, USA). The pore size distribution plots were obtained using the Barret-Joyner-Halenda (BJH) model.

Results and discussion

Morphology and structure

Uniform Cu_2O hollow spheres with rough surface were obtained by the simple one-step wet synthesis method. Figure 1 shows SEM images and diameter distributions of Cu_2O spheres prepared under different temperatures. It can be clearly observed that the sizes and structures of Cu_2O spheres changed under different conditions. When the reaction takes place in ice water bath keeping at 0°C, the obtained Cu_2O spheres are well distributed in size with a diameter of 763 ± 83 nm (Figure 1a,d). Few spherical particles are broken into pieces (inset of Figure 1a), so we can clearly find the hollow structure of the big sphere. The big sphere is made up of small particles, leaving nanoscale holes on the surface. At 25°C, the spheres are bigger in size with a diameter of 1,521 ± 73 nm (Figure 1b,e). In addition, the hollow structure

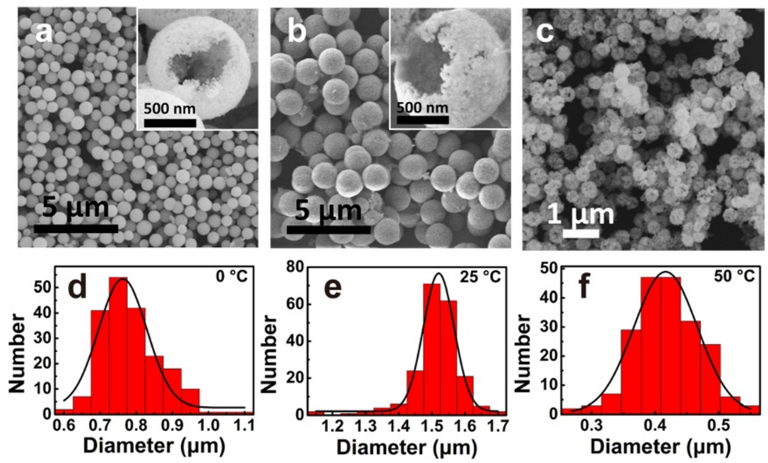

Figure 1 SEM images and particle size distribution. SEM images of Cu_2O hollow spheres obtained at 0°C **(a)**, 25°C **(b)**, and 50°C **(c)**. The insets show the corresponding hollow structures. Diameter distributions of Cu_2O hollow spheres prepared at 0°C **(d)**, 25°C **(e)**, and 50°C **(f)**.

can be easily observed from the broken sphere (inset of Figure 1b). However, when the reaction temperature increase to 50°C, the sphere morphology change a lot, which could hardly be called hollow sphere. Cu_2O spheres prepared at 50°C have rough surfaces with a diameter of 417 ± 51 nm (Figure 1c,f). The reaction time should be strictly controlled within 1 h to prepare Cu_2O spheres.

Figure 2 shows the TEM, high-resolution TEM (HRTEM), and selected area electron diffraction (SAED) images of Cu_2O spheres prepared under different temperatures. Figure 2a shows the morphology of Cu_2O spheres prepared at 0°C in which a hollow structure can be distinctly observed. The obtained Cu_2O spheres are uniform in size with a wall thickness of 130 nm. The hollow structure shown in Figure 2b can also be observed when the reaction temperature increases to 25°C. Figure 2c shows the morphology of Cu_2O spheres prepared at 50°C, in which nanoparticles aggregate together to form small sphere-like shape. A fringe spacing of 0.25 nm shown in the HRTEM images (Figure 2d,e,f) corresponds well to that of the lattice space of {111} of Cu_2O crystals.

The composition and phase purity of the products prepared at different reaction temperatures were characterized by XRD as shown in Figure 3. XRD patterns are confirmed with the SAED results, which show the expected (110), (111), (200), (220), (311), and (222) diffraction peaks corresponding to crystal planes of the Cu_2O crystals. The insets of Figure 2d,e,f show the SAED patterns of the obtained Cu_2O spheres, in which the

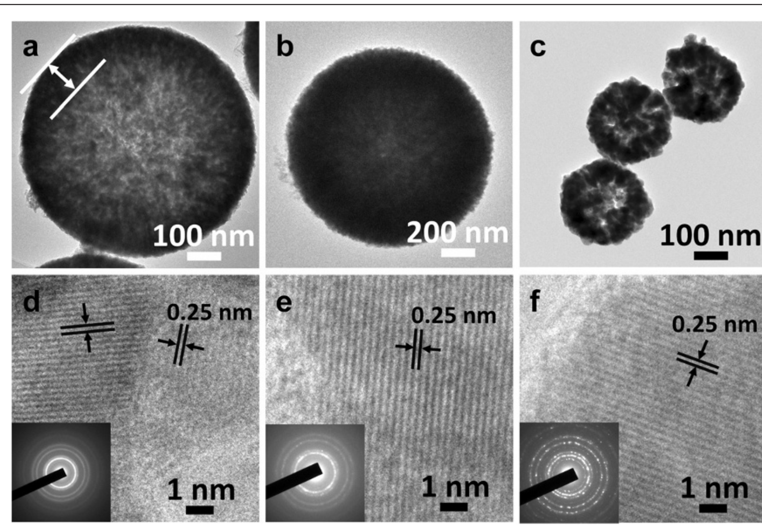

Figure 2 TEM and HRTEM images. TEM and HRTEM images of Cu_2O hollow spheres prepared at 0°C **(a, d)**, 25°C **(b, e)**, and 50°C **(c, f)**. The insets show the corresponding SAED patterns.

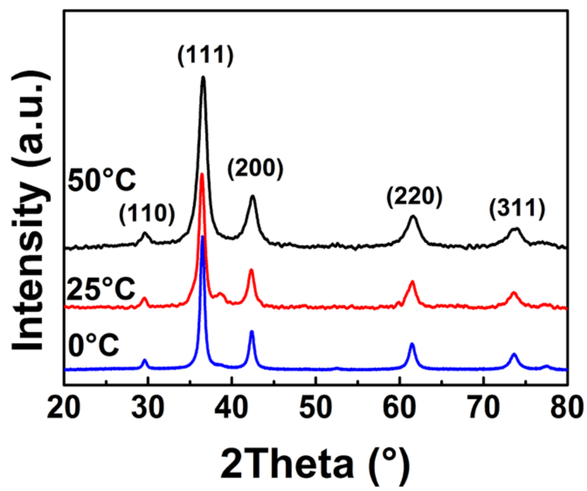

Figure 3 XRD patterns. XRD patterns of Cu_2O hollow spheres prepared at 0°C, 25°C, and 50°C.

diffraction rings fit well with crystal planes of Cu_2O. No other peak is observed in the XRD patterns, indicating that the products are phase-pure Cu_2O crystals. There is no impurity such as cupric oxide or copper.

Formation mechanism

Hydrazine hydrate ($N_2H_4 \cdot H_2O$) is used as the reductant to prepare Cu_2O hollow spheres. As $N_2H_4 \cdot H_2O$ is an alkali reductant with strong reducing ability, after injecting $N_2H_4 \cdot H_2O$, the solution turns into dark blue within several seconds and then changes to brick red gradually, which means that $Cu(OH)_2$ is generated and finally reduced to Cu_2O. The formation of Cu_2O hollow spheres in the reaction system can be represented by the following chemical reactions:

$$Cu^{2+} + 2OH^- = Cu(OH)_2$$

$$4Cu(OH)_2 + N_2H_4 = 2Cu_2O + 6H_2O + N_2$$

The process of morphology changing under different temperatures can be explained as the following steps in Figure 4.

At a certain temperature, for example, at 25°C, after the addition of $N_2H_4 \cdot H_2O$ into $CuSO_4$ solution, Cu^{2+} is reduced to Cu_2O nanoparticles, and N_2 nanobubbles are generated at the same time. As there is no surfactant in the reaction system, Cu_2O nanoparticles will tend to absorb on the surface of N_2 bubbles, so that Cu_2O nanoparticles assemble into hollow spheres (Figure 1a), which can be referred to the Ostwald ripening process [47]. When the reaction takes place at 0°C, the reaction rate will slow down, resulting in smaller N_2 bubbles and spheres with smoother surface and tighter structure, which also agrees with the SEM results and diameter distribution (Figure 1). The reaction rate increases along with the temperature rises. At 50°C, the reaction speed is too high for the nanoparticles to form uniform spheres. In Figure 1c, the hollow sphere structure could hardly be observed. N_2 nanobubbles escape faster so that the obtained Cu_2O spheres are smaller.

On the other hand, Cu_2O spheres are made up of nanoparticles. Crystallization rate increases with the rise of temperature to form bigger nanoparticles, so that the obtained Cu_2O spheres would have rougher surface, which is also in agreement with the SEM results (Figure 1).

Meanwhile, the morphology of Cu_2O hollow spheres changes during the reaction time. The SEM images obtained at 0°C during different formation times are displayed in Figure 5a,b,c,d. Hollow structures have been formed at 30 min but with inconsistent diameters. With the reaction time increase to 6 h, Cu_2O is oxidized into $Cu_4(OH)_6SO_4$ by oxygen dissolved in the solution, which can be confirmed by TEM and XRD results in Figure 5e,f.

Photocatalytic activities

A self-designed equipment was applied to carry out the photocatalytic degradation experiment as shown in Figure 6. Four 8-W LED lamps were used as cold light

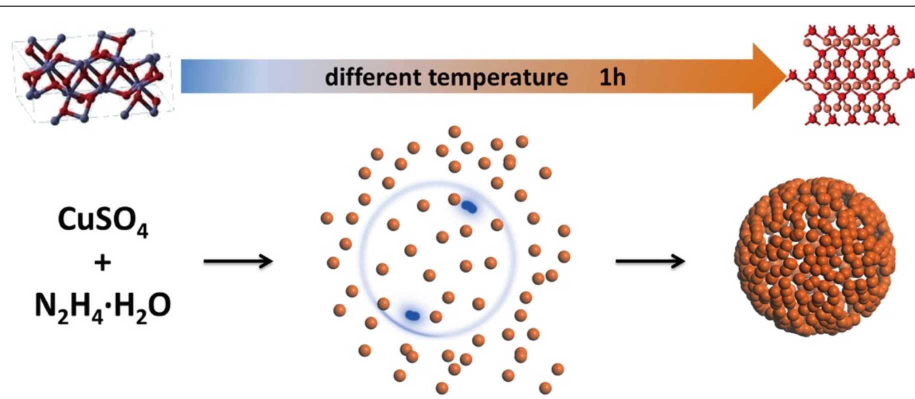

Figure 4 Schematic formation mechanism for bubble template process.

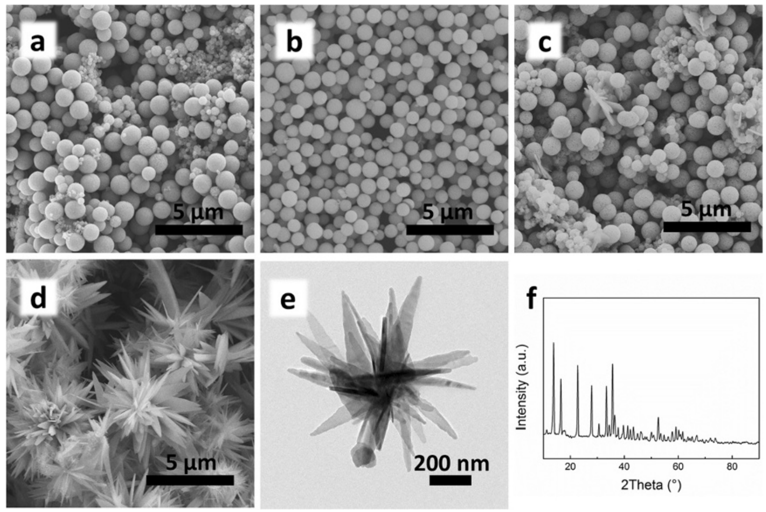

Figure 5 SEM images of formation process. SEM images of Cu_2O hollow spheres obtained at 0°C during different formation times (**(a)** 0.5 h, **(b)** 1 h, **(c)** 2 h, **(d)** 4 h). TEM image **(e)** and XRD pattern **(f)** of $Cu_4(OH)_6SO_4$.

sources which were mounted at 10 cm around the center of the reaction round-bottom flask. This equipment can ensure specific wavelength of the light with no heat introduced as LED lamps are cold light sources. We chose LED lamps with different characteristic wavelengths to serve as the light source of photocatalysis for the first time. LED lamps, as typical cold light sources, are different from Xe lamps with the power of 150 W and often used in the photocatalytic experiment. There is no extra heat introduced into the reaction system using LED cold light and the wavelength can be easily controlled. The LED lamps of wavelength 450, 550, and 700 nm were chosen as the visible light sources, as the limited experiment resources we have.

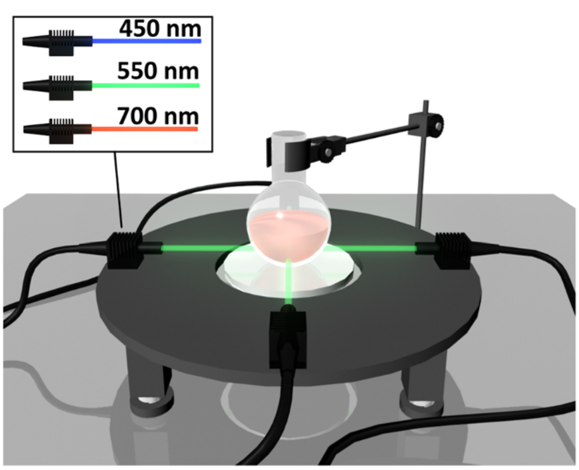

Figure 6 Schematic diagram of the self-designed photocatalytic equipment setup. The inset shows the figure of different LED lamps as cold light sources with a wavelength of 450, 550, and 700 nm, respectively.

To test the photocatalytic activities of obtained Cu_2O hollow spheres, MO, a negatively charged molecule, was used in the photodegradation experiments.

MO solution was kept in darkness for 15 min to get adsorption equilibrium. The adsorption curve in darkness is shown in Figure 7. It is found that adsorption have reached equilibrium after 15 min. Figure 8a,b,c,d,e,f shows the photocatalytic performance of Cu_2O as photocatalysts for the degradation of MO. The experimental results disclose that Cu_2O hollow spheres allow superior photocatalytic activity. Meanwhile, the time for concentration of MO solution to reach 1/*e* is summarized in Table 1, so we can have a clear look at the degradation of MO.

The results can be explained in two aspects, different wavelengths of visible lights and photocatalysts prepared

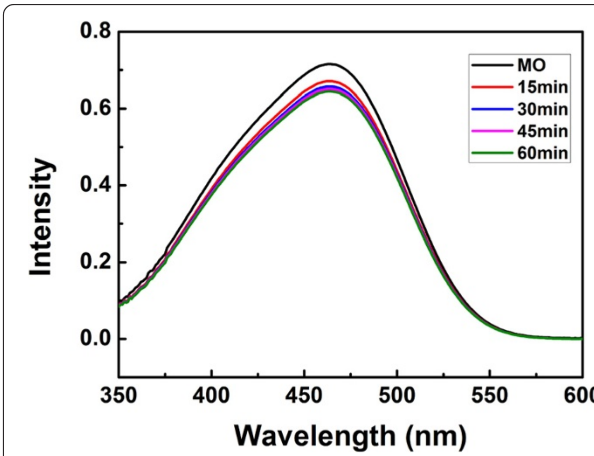

Figure 7 Adsorption effect of Cu_2O hollow spheres prepared at 0°C. The MO solution was kept in dark environment.

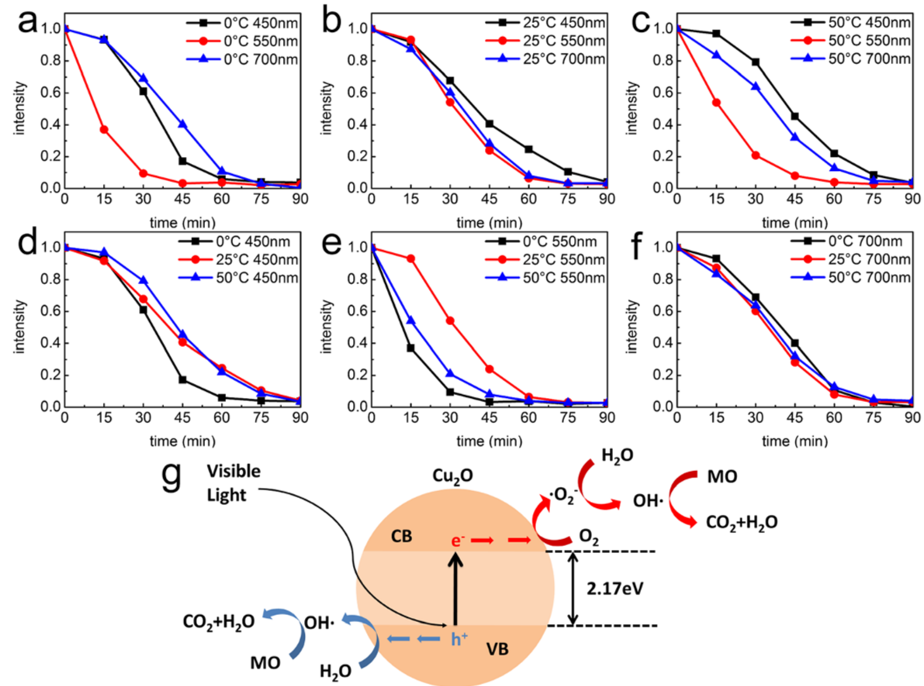

Figure 8 Degradation of MO in the presence of Cu_2O hollow spheres. Degradation of MO in the presence of Cu_2O hollow spheres prepared at different temperatures irradiated by different wavelengths of visible lights **(a-f)** and photocatalytic mechanism **(g)**.

at various temperatures. As shown in Figure 8a,b,c, the photocatalytic results indicate that the obtained Cu_2O spheres can photocatalyze MO degradation under visible light and the 550-nm wavelength light exhibits the most effective photocatalytic effect among all three spheres.

The light energy can be calculated using Einstein's photoelectric effect equation as follows:

$$E = h\frac{c}{\lambda}$$

In the equation, E represents the energy of light, h is the Planck's constant which equals 6.626×10^{-34}, c is the velocity of light, and λ refers to the experimental wavelength. When the photocatalytic reaction takes place under light of 550-nm wavelength, the energy is about 2.25 eV, which is very close to the band gap of Cu_2O (2.17 eV). Therefore, 550 nm is the most suitable wavelength for Cu_2O to photocatalytically degrade MO. At the same time, a contrast experimental result indicates that the MO solution will not be degraded without Cu_2O hollow spheres under different wavelengths (Figure 9).

Table 1 Time for the intensity of MO to achieve 1/*e*

Wavelength (nm)	Energy (eV)	Time to achieve 1/*e* (min)		
		0°C	25°C	50°C
450	2.75	28.27	48.67	50.49
550	2.25	15.03	33.64	22.86
700	1.77	46.67	40.09	42.67

As for different wavelengths of visible lights (450 and 550 nm), Cu_2O hollow spheres prepared at 0°C exhibit the highest degradation effect (Figure 8d,e), because Cu_2O spheres prepared at different temperatures possess different Brunauer-Emmett-Teller (BET) surface areas. N_2 adsorption-desorption isotherms (Figure 10) and the corresponding BJH pore size distribution plots (inset of Figure 10) of the obtained Cu_2O spheres are performed.

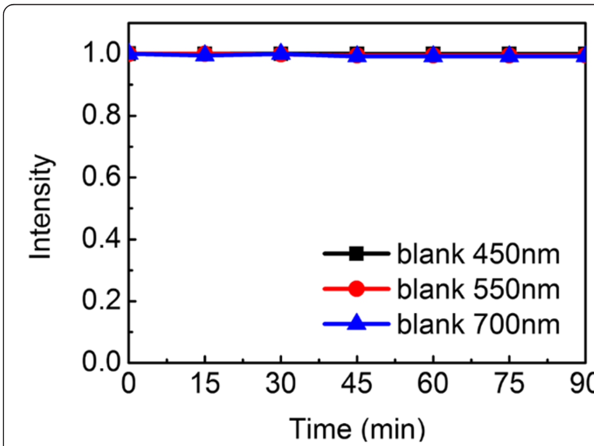

Figure 9 Contrast results without Cu_2O hollow spheres. The MO solution was kept in the same photocatalytic conditions without Cu_2O hollow spheres.

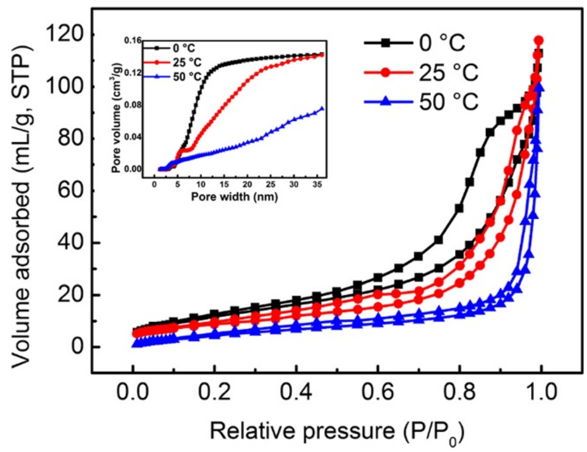

Figure 10 N_2 adsorption-desorption isotherm curves. N_2 adsorption-desorption isotherm curves of the different samples prepared at 0°C, 25°C, and 50°C. The inset shows the pore size distributions of the different samples.

It can be seen that the Cu_2O spheres prepared at 0°C have a relatively narrow pore size compared to the other two samples. Moreover, the BET surface area of the prepared Cu_2O spheres under 0°C (45.985 m^2/g) is larger than the surface areas of Cu_2O spheres under 25°C (31.961 m^2/g) and under 50°C (20.944 m^2/g). The larger BET surface area of the Cu_2O crystals can be attributed to the hollow structure and interconnected pores in the crystals.

The structure with larger BET surface area could facilitate effective contacts between Cu_2O spheres and organic contaminants, enhancing light harvesting and ultimately improving the photocatalytic activities. However, it shows almost the same effect under 700-nm wavelength among the three kinds of Cu_2O spheres (Figure 8f). Maybe under 700-nm wavelength LED lamps, the structure of spheres is not the dominant factor of the photocatalytic activities.

An illustration of inter-particle electron transfer behavior is proposed as shown in Figure 8g. The uniform distributions of Cu_2O hollow spheres have large active surface area, which enhances the effective adsorption of photons and provides a continuous pathway for the transportation of photoinduced electrons. The electrons in the valence band of Cu_2O are excited to its conducting band, giving rise to the formation of electron and hole pairs. The obtained electrons and holes with high energy can combine with H_2O and reduce MO into CO_2 and H_2O.

Conclusions

We demonstrate a facile method to prepare Cu_2O hollow spheres. Under the preparation at 0°C, 25°C, and 50°C, the obtained Cu_2O hollow spheres have diameters of 763 ± 83, 1,521 ± 73, and 417 ± 51 nm, respectively. The corresponding surface area is 45.985, 31.961, and 20.944 m^2/g, respectively. Cu_2O hollow spheres are obtained by nanoparticles absorbing on the surface of N_2 bubbles and assemble together. A bubble template process is introduced to explain the formation mechanism. Importantly, Cu_2O hollow spheres exhibit better photocatalytic activities for MO degradation under visible light. This is because the developed BET surface areas lead to more contact points, thus forming much more active sites between MO and the catalyst. So, Cu_2O hollow spheres prepared at 0°C are the most effective for the degradation of MO. At the same time, 550 nm is the most suitable wavelength for Cu_2O to photocatalytically degrade MO, because the light energy (2.25 eV) is closest to the band gap of Cu_2O (2.17 eV).

The work not only provides insights into the Cu_2O catalysis but is also useful for better catalyst design and water treatment industry. The LED lamps as cold light sources with no extra heat introduced into the reaction system are promoted in this work. In summary, we provide an efficient synthetic strategy for the fabrication of effective Cu_2O visible photocatalyst in environmental treatment, and the self-designed catalytic equipment with single-wavelength LED cold light sources exhibits a novel model for the catalytic design.

Competing interests

The authors declare that they have no competing interests.

Authors' contributions

YW performed most of the experiment and wrote the manuscript. DH and XZ helped analyze the characterization results. YM, HG, and YW maintained the self-designed photocatalytic equipment. GY and DH characterized the TEM and BET. ZY and NH supervised all of the study and provided financial support. All authors read and approved the final manuscript.

Acknowledgements

The authors gratefully acknowledge the financial support by the National Basic Research Program of China (2013CB932500), the National High-Tech R&D Program of China (863 program, 2011AA050504), the National Natural Science Foundation of China (51102164), the Program for New Century Excellent Talents in University (NCET-12-0356), and the Program for Professor of Special Appointment (Eastern Scholar) at Shanghai Institutions of Higher Learning. We also acknowledge the analysis support from the Instrumental Analysis Center of Shanghai Jiao Tong University.

Received: 11 October 2014 Accepted: 7 November 2014
Published: 22 November 2014

References

1. Wang W, Wang G, Wang X, Zhan Y, Liu Y, Zheng C: **Synthesis and characterization of Cu_2O nanowires by a novel reduction route.** *Adv Mater* 2002, **14:**67–69.
2. Cao M, Hu C, Wang Y, Guo Y, Guo C, Wang E: **A controllable synthetic route to Cu, Cu_2O, and CuO nanotubes and nanorods.** *Chem Commun* 2003, **15:**1884–1885.
3. Ho JY, Huang MH: **Synthesis of submicrometer-sized Cu_2O crystals with morphological evolution from cubic to hexapod structures and their comparative photocatalytic activity.** *J Phys Chem C* 2009, **113:**14159–14164.
4. Sui YM, Fu WY, Zeng Y, Yang HB, Zhang YY, Chen H, Li YX, Li MH, Zou GT: **Synthesis of Cu_2O nanoframes and nanocages by selective oxidative etching at room temperature.** *Angew Chem Int Ed* 2010, **49:**4282–4285.

5. Li JT, Cushing SK, Bright J, Meng F, Senty TR, Zheng P, Bristow AD, Wu NQ: Ag@Cu_2O core-shell nanoparticles as visible-light plasmonic photocatalysts. *ACS Catal* 2013, **3**:47–51.
6. Liu H, Zhou Y, Kulinich SA, Li JJ, Han LL, Qiao SZ, Du XW: Scalable synthesis of hollow Cu_2O nanocubes with unique optical properties via a simple hydrolysis-based approach. *J Mater Chem A* 2013, **1**:302–307.
7. Zhang L, Wang H: Cuprous oxide nanoshells with geometrically tunable optical properties. *ACS Nano* 2011, **5**:3257–3267.
8. Zhang HG, Zhu QS, Zhang Y, Wang Y, Zhao L, Yu B: One-pot synthesis and hierarchical assembly of hollow Cu_2O microspheres with nanocrystals-composed porous multishell and their gas-sensing properties. *Adv Funct Mater* 2007, **17**:2766–2771.
9. Xu LS, Chen XH, Wu YR, Chen CS, Li WH, Pan WY, Wang YG: Solution-phase synthesis of single-crystal hollow Cu_2O spheres with nanoholes. *Nanotechnology* 2006, **17**:1501–1505.
10. Lu CH, Qi LM, Yang JH, Wang XY, Zhang DY, Xie JL, Ma JM: One-pot synthesis of octahedral Cu_2O nanocages via a catalytic solution route. *Adv Mater* 2005, **17**:2562–2567.
11. Zhou ZH, Lin YL, Zhang PG, Ashalley E, Shafa M, Li HD, Wu J, Wang ZM: Hydrothermal fabrication of porous MoS_2 and its visible light photocatalytic properties. *Mater Lett* 2014, **131**:122–124.
12. Hu P, Yu LJ, Zuo AH, Guo CY, Yuan FL: Fabrication of monodisperse magnetite hollow spheres. *J Phys Chem C* 2009, **113**:900–906.
13. Chen ST, Zhang XL, Hou XM, Zhou Q, Tan WH: One-pot synthesis of hollow PbSe single-crystalline nanoboxes via gas bubble assisted Ostwald ripening. *Cryst Growth Des* 2010, **10**:1257–1262.
14. Siegfried MJ, Choi KS: Elucidating the effect of additives on the growth and stability of Cu_2O surfaces via shape transformation of pre-grown crystals. *J Am Chem Soc* 2006, **128**:10356–10357.
15. Siegfried MJ, Choi KS: Electrochemical crystallization of cuprous oxide with systematic shape evolution. *Adv Mater* 2004, **16**:1473–1476.
16. Bao HZ, Zhang ZH, Hua Q, Huang WX: Compositions, structures, and catalytic activities of CeO_2@Cu_2O nanocomposites prepared by the template-assisted method. *Langmuir* 2013, **30**:6427–6436.
17. Zhu YF, Ikoma T, Hanagata N, Kaskel S: Rattle-type Fe_3O_4@SiO_2 hollow mesoporous spheres as carriers for drug delivery. *Small* 2010, **6**:471–478.
18. Chen Y, Chen HR, Zeng DP, Tian YB, Chen F, Feng JW, Shi JL: Core/shell structured hollow mesoporous nanocapsules: a potential platform for simultaneous cell imaging and anticancer drug delivery. *ACS Nano* 2010, **4**:6001–6013.
19. Yao Y, McDowell MT, Ryu I, Wu H, Liu N, Hu LB, Nix WD, Cui Y: Interconnected silicon hollow nanospheres for lithium-ion battery anodes with long cycle life. *Nano Lett* 2011, **11**:2949–2954.
20. Zhang JZ: Biomedical applications of shape-controlled plasmonic nanostructures: a case study of hollow gold nanospheres for photothermal ablation therapy of cancer. *J Phys Chem Lett* 2010, **1**:686–695.
21. Niu KY, Yang J, Kulinich SA, Sun J, Du XW: Hollow nanoparticles of metal oxides and sulfides: fast preparation via laser ablation in liquid. *Langmuir* 2010, **26**:16652–16657.
22. Niu KY, Yang J, Kulinich SA, Sun J, Li H, Du XW: Morphology control of nanostructures via surface reaction of metal nanodroplets. *J Am Chem Soc* 2010, **132**:9814–9819.
23. An K, Hyeon T: Synthesis and biomedical applications of hollow nanostructures. *Nano Today* 2009, **4**:359–373.
24. Xu HL, Wang WZ, Zhu W: Shape evolution and size-controllable synthesis of Cu_2O octahedra and their morphology-dependent photocatalytic properties. *J Phys Chem B* 2006, **110**:13829–13834.
25. Zhang JT, Liu JF, Peng Q, Wang X, Li YD: Nearly monodisperse Cu_2O and CuO nanospheres: preparation and applications for sensitive gas sensors. *Chem Mater* 2006, **18**:867–871.
26. Zhang N, Du YL, Zhang Y, Wang CM: A simple method for controlling the type of cuprous oxide semiconductors using different surfactants. *J Mater Chem* 2011, **21**:5408–5013.
27. Diab M, Moshofsky B, Plante IJ, Mokari T: A facile one-step approach for the synthesis and assembly of copper and copper-oxide nanocrystals. *J Mater Chem* 2011, **21**:11626–11630.
28. Liu YB, Zhou HB, Li JH, Chen HC, Li D, Zhou BX, Cai WM: Enhanced photoelectrochemical properties of Cu_2O-loaded short TiO_2 nanotube array electrode prepared by sonoelectrochemical deposition. *Nano-Micro Lett* 2010, **2**:277–284.
29. Wang WZ, Huang XW, Wu S, Zhou YX, Wang LJ, Shi HL, Liang YJ, Zou B: Preparation of p-n junction $Cu_2O/BiVO_4$ heterogeneous nanostructures with enhanced visible-light photocatalytic activity. *Appl Catal B Environ* 2013, **134**:293–301.
30. Kuo CH, Huang MH: Morphologically controlled synthesis of Cu_2O nanocrystals and their properties. *Nano Today* 2010, **5**:106–116.
31. Kim MH, Lim B, Lee EP, Xia YJ: Polyol synthesis of Cu_2O nanoparticles: use of chloride to promote the formation of a cubic morphology. *J Mater Chem* 2008, **18**:4069–4073.
32. Zhang H, Ren X, Cui Z: Shape-controlled synthesis of Cu_2O nanocrystals assisted by PVP and application as catalyst for synthesis of carbon nanofibers. *J Cryst Growth* 2007, **304**:206–210.
33. Liang X, Gao L, Yang S, Sun J: Facile synthesis and shape evolution of single-crystal cuprous oxide. *Adv Mater* 2009, **21**:2068–2071.
34. Huang L, Peng F, Yu H, Wang H: Preparation of cuprous oxides with different sizes and their behaviors of adsorption, visible-light driven photocatalysis and photocorrosion. *Solid State Sci* 2009, **11**:129–138.
35. Kuo C-H, Huang MH: Fabrication of truncated rhombic dodecahedral Cu_2O nanocages and nanoframes by particle aggregation and acidic etching. *J Am Chem Soc* 2008, **130**:12815–12820.
36. Siegfried MJ, Choi K-S: Directing the architecture of cuprous oxide crystals during electrochemical growth. *Angew Chem* 2005, **117**:3282–3287.
37. Somasundaram S, Chenthamarakshan CRN, de Tacconi NR, Rajeshwar K: Photocatalytic production of hydrogen from electrodeposited p-Cu_2O film and sacrificial electron donors. *Int J Hydrogen Energy* 2007, **32**:4661–4669.
38. Singh DP, Neti NR, Sinha ASK, Srivastava ON: Growth of different nanostructures of Cu_2O (nanothreads, nanowires, and nanocubes) by simple electrolysis based oxidation of copper. *J Phys Chem C* 2007, **111**:1638–1645.
39. Xu Y, Jiao X, Chen D: PEG-assisted preparation of single-crystalline Cu_2O hollow nanocubes. *J Phys Chem C* 2008, **112**:16769–16773.
40. Teo JJ, Chang Y, Zeng HC: Fabrications of hollow nanocubes of Cu_2O and Cu via reductive self-assembly of CuO nanocrystals. *Langmuir* 2006, **22**:7369–7377.
41. Zhang H, Zhang X, Li H, Qu Z, Fan S, Ji M: Hierarchical growth of Cu_2O double tower-tip-like nanostructures in water/oil microemulsion. *Cryst Growth Des* 2007, **7**:820–824.
42. He P, Shen X, Gao H: Size-controlled preparation of Cu_2O octahedron nanocrystals and studies on their optical absorption. *J Colloid Interface Sci* 2005, **284**:510–515.
43. Chen Q, Shen X, Gao H: Formation of solid and hollow cuprous oxide nanocubes in water-in-oil microemulsions controlled by the yield of hydrated electrons. *J Colloid Interface Sci* 2007, **312**:272–278.
44. Meng XY, Tian GH, Chen YJ, Qu Y, Zhou J, Pan K, Zhou W, Zhang GL, Fu HG: Room temperature solution synthesis of hierarchical bow-like Cu_2O with high visible light driven photocatalytic activity. *RSC Adv* 2011, **2**:2875–2881.
45. Su XD, Zhao JZ, Bala H, Zhu YC, Gao Y, Ma SS, Wang ZC: Fast synthesis of stable cubic copper nanocages in the aqueous phase. *J Phys Chem C* 2007, **111**:14689–14693.
46. Wang WZ, Zhang PC, Peng L, Xie WJ, Zhang GL, Tu Y, Mai WJ: Template-free room temperature solution phase synthesis of Cu_2O hollow spheres. *Cryst Eng Comm* 2010, **12**:700–701.
47. Jin L, Xu LP, Morein C, Chen CH, Lai M, Suib SL: Titanium containing γ-MnO_2 (TM) hollow spheres: one-step synthesis and catalytic activities in Li/air batteries and oxidative chemical reactions. *Adv Funct Mater* 2010, **20**:3373–3382.

doi:10.1186/1556-276X-9-624
Cite this article as: Wang *et al.*: Surfactant-free synthesis of Cu_2O hollow spheres and their wavelength-dependent visible photocatalytic activities using LED lamps as cold light sources. *Nanoscale Research Letters* 2014 **9**:624.